Isotopic quantum effects in water structure measured with high energy photon diffraction

2000 J. Phys.: Condens. Matter 12 2597

(http://iopscience.iop.org/0953-8984/12/12/303)

J. Phys.: Condens. Matter **12** (2000) 2597–2612. Printed in the UK PII: S0953-8984(00)10138-9

Isotopic quantum effects in water structure measured with high energy photon diffraction

B Tomberli†, C J Benmore‡, P A Egelstaff†, J Neuefeind§ and V Honkimäki‖

† Department of Physics, University of Guelph, Guelph, Ontario, Canada N1G 2W1
‡ ISIS Facility, CLRC Rutherford Appleton Laboratory, Chilton, Oxfordshire OX11 0XQ, UK
§ HASYLAB at DESY, Notkestrasse 85, 22603 Hamburg, Germany
‖ European Synchrotron Radiation Facility, BP 220, F-38043 Grenoble Cedex, France

Received 7 December 1999

Abstract. High energy electromagnetic radiation scattering techniques have been used to measure the structural differences between light and heavy water: we have studied both intra- and intermolecular effects. These methods and our data analysis are described in detail. We have observed a maximum isotopic effect of 1.6% relative to the magnitude of the x-ray structure factor. Our uncertainties are an order of magnitude smaller than those of previous γ-ray measurements (Root J H, Egelstaff P A and Hime A 1986 *Chem. Phys.* **109** 5164) and this has permitted us to test accurately the available quantum simulation results on water. The SPC and TIP4P potentials reproduce the measured results in r-space moderately well for intermolecular effects at distances greater than 2.5 Å. These results show that H_2O is a slightly more disordered liquid than D_2O at the same temperature.

(Some figures in this article appear in colour in the electronic version; see `www.iop.org`)

1. Introduction

The theoretical study of molecular liquids involves various approximations: most often it is assumed that at room temperature they are composed of classical, rigid molecules interacting via a pair potential. The validity of such simplifications for hydrogenous liquids is challenged by the fact that their bulk properties show isotopic variations. For example, the melting and boiling points are higher for D_2O than H_2O [2], which suggests that the quantum-mechanical nature of these molecules is responsible for a measureable effect, even at room temperature. This idea is not new: for example, it has long been believed [3] that D_2O is a slightly more structured liquid than H_2O at room temperature. This was first demonstrated experimentally by the low intensity γ-ray experiments of Root *et al* [1], who exploited the properties of high energy radiation in reducing experimental corrections. Although they were successful in measuring a small isotopic effect upon the fluid structure, the accuracy of their work was limited by statistical errors. Furthermore their results disagreed in magnitude with the available calculations of structural differences determined by path-integral Monte Carlo quantum simulations [4]. With the advent of powerful synchrotron sources, such measurements can be improved substantially and thus more precise experiments have become possible. A general discussion of the structure of water has been given by Narten and Levy [5].

Our objective is to determine quantitatively the structural differences between light and heavy water at the same temperature and at atmospheric pressure. We note that under these conditions, quantum isotopic effects force quantities such as the structural parameters and the

0953-8984/00/122597+16$30.00

number densities of H_2O and D_2O to differ slightly (see tables 1 and 2). We intend to improve the quality of existing electromagnetic radiation scattering measurements [1] by using high intensity beams of (approximately) 110 keV synchrotron radiation together with lower angles of scatter.

Isotopic difference measurements have been used in neutron diffraction hydrogen–deuterium substitution experiments, wherein the first order difference in the intermolecular structure between isotopic samples is usually assumed to be zero [6]. If the intermolecular H and D structures in water show small differences, a useful property to investigate would be the possibility of a temperature shift that would minimize those differences. If successful, this technique may be useful with other experiments on water (e.g. the velocity of sound [7] etc). We note, however, that intramolecular effects would not be minimized by a temperature shift that minimizes intermolecular effects and we shall demonstrate this point. Moreover, our experiments provide a rigorous test of the intermolecular potentials used in quantum-mechanical calculations for water [4,8]. The largest corrections to the classical model of molecular interactions are believed to be caused by the coupling of intra and inter modes via hydrogen bonding [9], by differences in their ground state librations [9] and by many-body effects [10]. Agreement of a particular model with our measured results would help to establish its validity in estimating such effects. Again we note that these models [4,8] do not include intramolecular effects while the experimental data do. As the precision of many other experiments on water is improved, one may expect that our high precision structure results will find many other uses.

2. Theoretical development

The structure of a molecular liquid is usually described by a set of site–site partial pair distribution functions, $g_{\alpha\beta}(r)$. A partial pair distribution function is the ratio of the local number density to the bulk number density around an arbitrarily chosen central atom. There are three such partial functions in the case of water: $g_{OO}(r)$, $g_{OH}(r)$ and $g_{HH}(r)$. These partials are related to an intermolecular partial site–site structure factor, $D_{\alpha\beta}(Q)$, by a Fourier transform relation [11]:

$$D_{\alpha\beta}(Q) = \rho \int \mathrm{d}\boldsymbol{r} \exp(\mathrm{i}\boldsymbol{Q}\cdot\boldsymbol{r})[g_{\alpha\beta}(r) - 1] \tag{1}$$

where ρ is the molecular density and $Q = 4\pi \sin(2\theta)/\lambda$ is the momentum transfer given by the scattering angle, 2θ, and the wavelength of the incident radiation, λ. A diffraction experiment will not directly observe the partial structure factors but rather a sum of their weighted averages. For electromagnetic scattering if one uses the approximation that each atom scatters radiation independently then the total intermolecular electronic structure factor is [5]:

$$D_X(Q) = f_O^2(q)D_{OO}(Q) + 4f_O(Q)f_H(Q)D_{OH}(Q) + 4f_H^2(q)D_{HH}(Q) \tag{2}$$

where the Q-dependent atomic form factors, f_α, are the Fourier transforms of the electronic wave functions over all space for a single free atom of type α. They are tabulated in the literature [12]. We note here that equation (2) was used to generate estimates of $D_X(Q)$ from computer simulation results [4,8,10] and consequently the theoretical $D_X(Q)$ results depend on the independent atom approximation (IAA). However, we estimate that the error in the isotopic difference due to the IAA is proportional to the isotopic difference in the individual errors, which is much smaller than the error in the approximation itself. We note that $D_X(Q)$ is related to the structure factor, $S_X(Q)$, by the simple equation:

$$D_X(Q) = S_X(Q) - \langle F^2 \rangle \tag{3a}$$

where $\langle F^2 \rangle$ is the intramolecular scattering. Furthermore, the structure factor, $S_X(Q)$, can be calculated from $I_X(Q)$, the intensity measured in a diffraction experiment, and the Compton scattering $C_X(Q)$:

$$S_X(Q) = I_X(Q) - C_X(Q). \tag{3b}$$

The quantity $\langle F^2 \rangle$ is approximately that for isolated single molecules [14] and can be determined using the independent atom approximation [ ]. Again, our use of the IAA is reasonable because we use it only at high Q, where it is very good, in order to calibrate the structure factor of each isotope. Then we shall take the isotopic difference in structure factors: therefore only the difference in the errors of the high Q calibrations of the $S_X(Q)$s is introduced by our use of the IAA. This quantity is much smaller than the error in the IAA, which for the water $S(Q)$ in the vapour phase is less than 1% [13]. Therefore, the error in our differences will be much less than the high Q error in the IAA. For a molecule of known structure, the intramolecular scattering $\langle F^2 \rangle$ is then given by

$$\langle F^2 \rangle = \sum_i \sum_j f_i f_j \frac{\sin r_{ij} Q}{r_{ij} Q} \exp^{-b_{ij} Q^2}. \tag{4}$$

The summation is over all scattering centres in the molecule, each with spatial separation r_{ij} and positional variances b_{ij}. The structural quantities for H_2O and D_2O required in equation (4) are provided in table 1: the errors in these quantities are difficult to estimate from available data and the origins of our error estimates are given below the table.

Table 1. Structural parameters for H_2O and D_2O [15].

	H_2O	D_2O
O–H bond length (Å)	0.9724 ± 0.0006[a]	0.9686 ± 0.0006
H–O–H bond angle	104.63 ± 0.05[a]	104.57 ± 0.05[a]
H–H distance (Å)	1.539 ± 0.002[a]	1.532 ± 0.002[a]
O–H variance (Å^2)	0.0023 ± 0.0002[b]	0.0017 ± 0.0002[b]
H–H variance (Å^2)	0.0082 ± 0.001[b]	0.006 ± 0.001[b]

[a] These errors are estimated from table XI in [15].
[b] These errors are estimated from differences between [15] and [16].

$C_X(Q)$ in equation (3) is the Compton scattering which can be found to a good approximation by summing the atomic contributions which are tabulated in the literature [12]. As Q increases, $C_X(Q)$ asymptotically approaches the number of electrons, with relativistic corrections as given by the Klein–Nishina formula [12,17]. As will be seen in section 4 (Data reduction), this property can be used to normalize $S_X(Q)$ in units of electrons per molecule. The scattering per molecule, $i(Q)$, is obtained from the equation:

$$i(Q) = \frac{S_X(Q)}{\sum_i f_i(Q=0)} \tag{5}$$

where $\sum_i f_i(Q=0)$ is the total number of electrons in the molecule. This intensity can be inverse transformed to yield a total electronic correlation function [18]:

$$g_X(r) = 1 + \frac{1}{2\pi^2 \rho r} \int Q i(Q) \sin(Qr) \mathrm{d}Q \tag{6}$$

and

$$g_X(r) \to 0 \quad \text{as} \quad r \to 0$$

where ρ is the electronic density per Å^3. The X subscript indicates that the electronic structure factor was used to derive the correlation function. The difference between measurements on

H and D compounds will be denoted by $\Delta g_X(r)$ and from (6) we see that $\Delta g_X(r) \to 0$ as $r \to 0$.

Interestingly, if a neutron diffraction experiment is performed, it is possible to uniquely determine all of the partial correlation functions of water (to a first approximation) by the technique of isotopic substitution [6]. This technique exploits the fact that different isotopes have different neutron scattering cross sections to get a system of equations each similar to equation (2). This system can be solved to yield the partial correlation functions. An underlying assumption of the technique is that all the different isotopic samples have the same liquid structure. Unlike neutron scattering cross sections, atomic scattering cross sections for electromagnetic radiation are nearly isotope independent because they depend upon the electron density surrounding the nucleus (which is almost the same for atoms of differing isotopes). Therefore, E-M radiation scattering experiments are sensitive to the small isotopic differences in the intermolecular structure, and therefore can set a limit upon the structural variations ocurring through isotopic substitution in molecular fluids and thus test the assumptions used in neutron scattering experiments.

3. Experimental details

To measure isotopic substitution effects accurately, it is necessary to perform experiments to a relative accuracy of 0.25% or better. In order to demonstrate whether this had been achieved, four separate experiments were carried out on two different instruments on different sources. Three experiments were conducted on the diffractometer on the BW5 wiggler beamline [19] on the DORIS III storage ring at DESY in Hamburg, Germany and one measurement was performed on an apparatus we constructed on the ID15A beamline at ESRF in Grenoble, France. Diagrams of the experimental set-ups (slit openings, relevant lengths, beam dimensions etc) are provided in figure 1 (HASYLAB with July 98 settings) and figure 2 (ESRF). At HASYLAB a vacuum tank surrounded the sample to suppress air scattering. To eliminate air scattering at ESRF special care was taken to ensure that the slits directed a collimated beam on the scattering centre while shadowing as little of the sample as possible. Table 2 entabulates other relevant differences between the four experiments. Unless stated otherwise all quantities have an uncertainty of ± 1 in the last digit: e.g. the number density error is $\pm 10^{-5}$ molecules Å^{-3}.

Table 2. Experimental summary.

	HASYLAB—BW5			ESRF—ID15A
Data	July 98	February 99	September 99	July 98
Sample temperature	27.5 ± 0.5 °C	22.3 ± 0.25 °C	25.7 ± 0.1 °C	23.5 ± 0.25 °C
H_2O number desnity	0.03334 molecules Å^{-3}	0.03338 molecules Å^{-3}	0.03336 molecules Å^{-3}	0.03337 molecules Å^{-3}
D_2O number density	0.03324 molecules Å^{-3}	0.03328 molecules Å^{-3}	0.03326 molecules Å^{-3}	0.03327 molecules Å^{-3}
Beam energy	101.87 keV	120.7 keV	100.0 keV	116.2 keV
Beam wavelength	0.1218 Å	0.1028 Å	0.1241 Å	0.1068 Å
Beam polarization	91% horizontal	91% horizontal	91% horizontal	90% horizontal
Q range	0.56–17.9 Å^{-1}	0.61–26.0 Å^{-1}	0.61–17.6 Å^{-1}	0.49–20.2 Å^{-1}

The same general precautions in both experiments reduced attenuation, multiple scattering and other corrections within the sample compared to conventional x-ray experiments. To

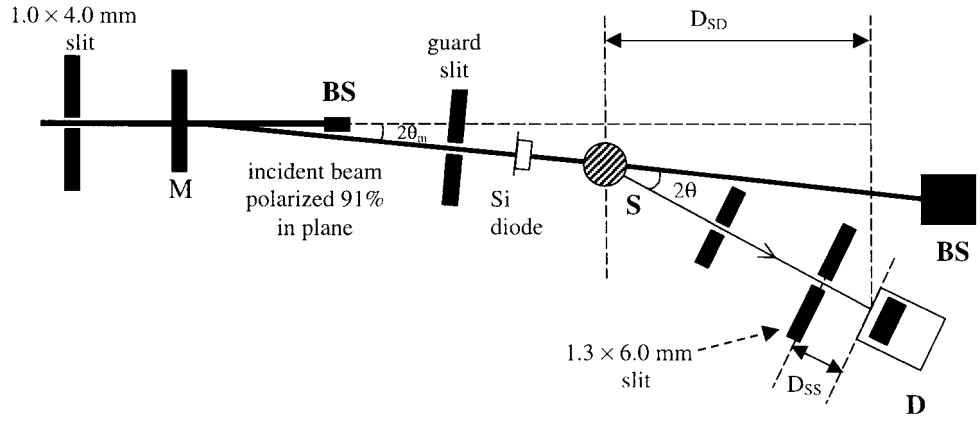

Figure 1. Schematic diagram of BW5 diffractometer at HASYLAB. S denotes the sample position, M the monochromator, BS the beam stop and D the liquid N_2 cooled Ge detector. The distances: $D_{SD} = 1557.5$ mm, $D_{SS} = 365.5$ mm, Bragg's angle $\theta_m = 1.1115°$ are for the geometric correction in equation (8).

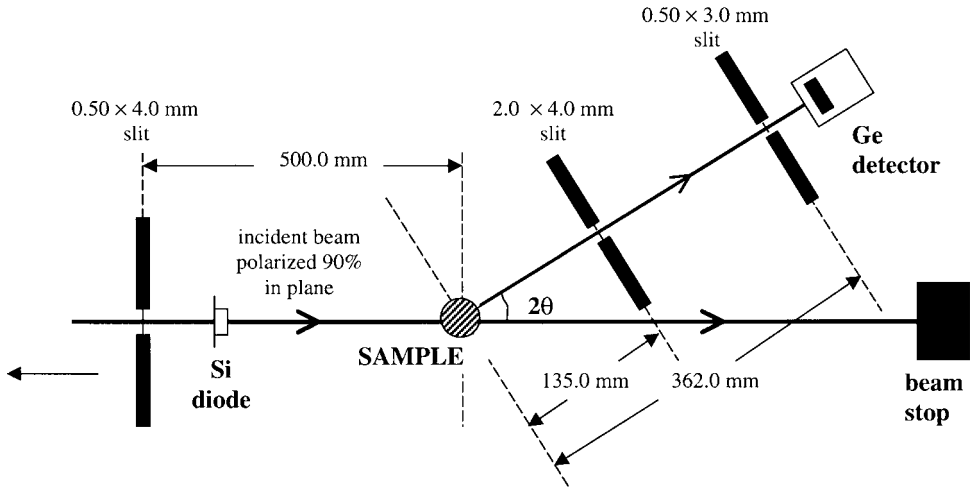

Figure 2. Schematic diagram of diffraction apparatus set-up at ESRF beamline ID15A.

reduce vessel scattering, all experiments used thin walled (10 μm) silica tubes of 2–3 mm diameter (supplier: GLAS Müller, D-13503 Berlin) to hold liquid water. Isotopically pure H_2O ($D_2O < 0.00015\%$) and isotopically purified D_2O (99.7% D_2O) were used as samples (the supplier for both was Aldrich). The samples were contained in pairs of matched silica tubes ranging in diameter from 2 to 3 mm fixed rigidly onto a translation table. Transmission x-ray scans were used to locate the tube centres for both the sample and empty vessel runs and their positions were found to be reproducible within 0.1 mm. After placing a sample in each tube, the opening of each tube was sealed with parafilm and coated with epoxy to keep the sample free of atmospheric contamination and prevent sample loss. The beams, with widths of 1.00 mm (HASYLAB) and 0.5 mm (ESRF), were centred on the sample tubes. For the 3.00 mm tubes 5% of the beam was scattered, and for the 2.00 mm tube 3.5% of the beam

was scattered. The ratio of sample to vessel scattering was approximately 11 at 2 Å^{-1} for all experiments. The sample plus vessel and empty vessel scattering was collected in a series of runs. Because the beam current at both ESRF and HASYLAB varied with time, the intensity incident on the sample was also monitored using a photodiode placed after the last collimating slit but far enough in front of the sample to avoid scattering from it. Beam variation and other time dependent effects were reduced by interleaving many scans on each isotope. As can be seen in figures 1 and 2, both experiments used radiation that was polarized out of the scattering plane. The polarization correction, P, was defined using the following formula [20],

$$P = \frac{1}{F_{ver} + F_{hor}\cos^2(2\theta)} \tag{7}$$

where the F_{ver} and F_{hor} denote the fraction polarized in the vertical and horizontal directions, respectively and are given in table 2. In the case of the translational scanning diffractometer arm at HASYLAB, an additional geometric correction was required to the data, namely:

$$g_k = \left(\frac{[D_{SD}/\cos(2\theta_m)] - D_{SS}}{[D_{SD}/\cos(2\theta_m + 2\theta)] - D_{SS}}\right)^2 \tag{8}$$

where the quantities are as shown in figure 1. At the ESRF, Bragg peaks from a 99.999% pure Al sample were used to calibrate the angular scale. Both experiments required a small adjustment (less than 0.006 Å^{-1}) to the horizontal scale to correct for the width of the angle of scatter [21].

4. Data reduction

The beam intensity from both sources is very high and therefore the raw detector counts required a correction for detector deadtime. The count rate entering a detector, I_c, is related to the true number of counts, I_0, by the expression:

$$I_c = I_0 \exp(-I_0\tau) \tag{9}$$

where τ is the deadtime of the detector. At HASYLAB, the deadtime was determined by two different methods. In the first method, τ was adjusted until all scans of a given sample in the same tube, which differ in count rate only due to the intensity variation of the incident radiation, gave the same intensity. In this manner the deadtime for the July 98 HASYLAB experiment was found to be $\tau = 2.04\ \mu\text{s}^{-1}$. In the second method deadtime was determined by placing 16 iron attenuators of different thickness, z, in the beamline to generate a series of points with a known intensity variation,

$$I_0 = I_i \exp(-\beta z) \tag{10}$$

where β is the extinction coefficient for iron and I_i is the incident beam energy. From equation (10) it is clear that a plot of $\exp(-\beta z)/I_0$ against z will yield a constant for the correct deadtime (the incident beam energy varies over a period of $\sim$ 12 h; the attenuation experiment takes about 60 s). Trial values of I_0 were found by using a bisection method to solve equation (10) for an estimated deadtime. The average and standard deviation of all 16 points in the resulting $\exp(-\beta z)/I_0$ against z curve was determined. The deadtime was varied until the standard deviation was minimized, resulting in the flattest shape for all values of z. In this manner the deadtime was found to be $\tau = 2.02\ \mu\text{s}^{-1}$ in the February 99 experiment and $\tau = 2.51\ \mu\text{s}^{-1}$ in September of 1999. Once τ is known, equation (9) is used determine I_0 for each measured count rate, I_c.

At ESRF the aperature of a shutter, approximately 10 m in front of the sample was varied, producing a variation in the incident radiation. Because the beam at ESRF has a Gaussian profile (FWHM = 3.92 mm), the measured intensity adjusted for beam profile, namely:

$$I_e = \left(I_c \Big/ \int_X \exp(-bx'^2) \mathrm{d}x' \right) \tag{11}$$

will vary linearly with X at low count rates. Due to deadtime in the detector, I_e will lie increasingly below the extrapolation of the I_e against X line, found from small values of X, as X (and therefore the count rate) increases. Using this extrapolation from small X values (and low count rate) to generate the true value for I_e at larger values of X (and hence higher count rates), a response curve relating the measured I_e to the true deadtime corrected I_e is found. This response curve was applied to relate the counted rate I_c to the true number of counts I_0 in a diffraction experiment.

The following definitions are useful for discussing the conversion of the data into absolute units, where S indicates sample and V indicates vessel:

- I_0^{SV} and I_0^V are count rates from the sample plus vessel and empty vessel systems, corrected for beam intensity, polarization, geometric effects, angle of scatter [21] and deadtime.
- B is background count rate measured with the beam on but no sample or vessel in its path.
- M_{SV} is the multiple scattering estimate from the sample plus vessel system [22]. Multiple scattering from the vessel alone is effectively zero.
- N_S and N_V are numbers of molecules of sample and vessel illuminated by the beam.
- σ_{SV} is the scattering cross section for the sample plus vessel system.
- $A_{i,jk}$ is a self-absorption factor for scattering in body i, and absorption in bodies j and k.
- $b = e^2/mc^2$ is the classical radius for an electron.
- $S_S(Q)$ and $S_V(Q)$ are the single scattering contributions from the sample and vessel as defined by equation (3).

The empty vessel scattering intensity can then be expressed, in terms of a constant [1], a,

$$I_0^V = B + a\{A_{V,V} N_V b^2 S_V(Q)\}. \tag{12}$$

For the sample plus vessel system, the expression for the scattered intensity [1] is,

$$I_0^{SV} = B + a\left\{ A_{S,SV} N_S b^2 \left(S_S(Q) + \frac{\sigma_{SV}}{4\pi b^2} M_{SV} \right) + A_{V,SV} n_V b^2 S_V(Q) \right\}. \tag{13}$$

Combining equations (12) and (13) an expression for the single scattering from the sample is obtained:

$$I_X(Q) = K\left(\frac{I_0^{SV} - B}{A_{S,SV}} - \frac{A_{S,SV}(I_0^V - B)}{A_{S,SV} A_{V,V}} \right) - \frac{\sigma_{SV}}{4\pi b^2} M_{SV} \tag{14}$$

where $K = (aN_S b^2)^{-1}$. Because each tube differed slightly, it was necessary to calculate the calibration constant, K, for each tube and sample system separately. This constant is found by using the fact that $D_X(Q)/S_X(Q) < 0.001$ for $Q > 10$ Å^{-1}. Therefore we may find the constant, K, from equation (3b) in the limit $Q > 10$ Å^{-1}, where $I_X(Q) \cong \langle F^2 \rangle + C_X(Q)$ and $\langle F^2 \rangle$ can be calculated using equation (4) (the independent atom approximation) and $C_X(Q)$ from the Klein–Nishina formula [12].

The multiple scattering correction was found using a method described in [22]. The resulting values were $M_{SV} = 0.013$, 0.008 and 0.014 for the July 98, February 99 and September 99 experiments at HASYLAB, respectively and $M_{SV} = 0.003$ at ESRF. The correction for self-attenuation was found using a method similar to that of [23] resulting in the values of: $A_{S,SV} = A_{V,SV} = 0.959$ and $A_{V,V} = 1.000$ for all experiments. The difference in

these quantities for light and heavy water is $\sim 10^{-4}$. Solving for A using the $Q > 10$ Å^{-1} data, $S_X(Q)$ can thus be determined in absolute electron units for both H_2O and D_2O over the entire measured range. The H_2O–D_2O difference was extended to the range $0 < Q < 0.6$ Å^{-1} from the lowest experimental points, using a maximum entropy procedure [24], to force agreement with the known values of $S_X(0)$ for H_2O and D_2O [25].

A maximum statistical variation of less than 0.5% in the region of the main peak for H_2O was observed between scans of the same sample in the same tube. After averaging over 12 scans per sample at HASYLAB (July 98, February 99 and September 99) and 13 at ESRF, final statistical errors of approximately 0.14% were obtained from each instrument. Averaging the two experimental results reduces the statistical error to 0.1%, which is small enough to observe isotopic effects over a wide range of Q values.

5. Results

Figure 3 shows $S_X(Q) - C_X(Q)$ at an effective temperature of 25.5 °C for light water averaged from our HASYLAB (July 98) and ESRF (July 98) data (over the range of greatest interest) compared to the x-ray measurements by Narten and Levy [14] at 25 °C. For $Q < 1.2$ Å^{-1}, the disagreement of our data (which were calibrated absolutely) with that of Narten and Levy, is caused by their fitting the low Q data to the $Q = 0$ isothermal compressibility limit. Also, our data are a little higher for 2.5 Å^{-1} $< Q <$ 3.0 Å^{-1}. Such small observable differences

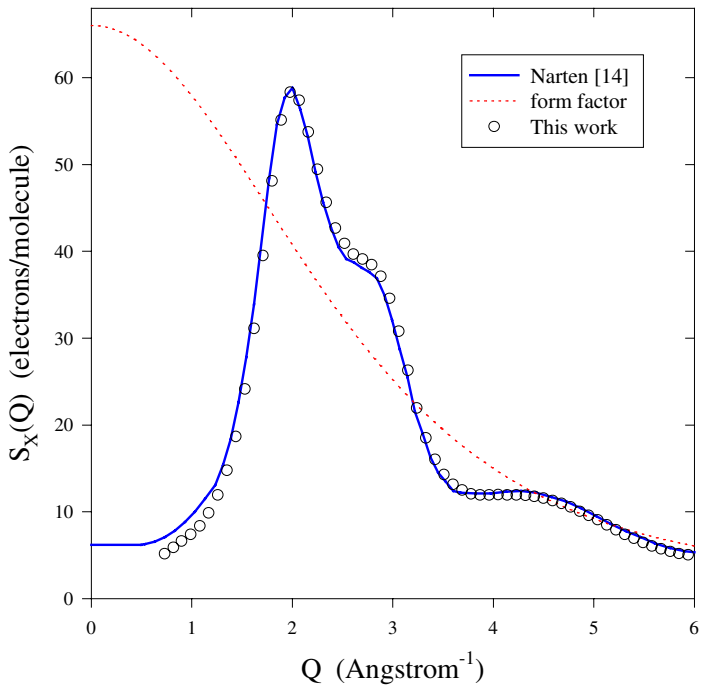

Figure 3. The static structure factor, $S_X(Q)$, for H_2O averaged over measurements from HASYLAB at $T = 27.5$ °C and ESRF at 23.5 °C (circles) compared to $S_X(Q)$ for H_2O measured by Narten and Levy [14] (solid line). The independent atom model form factor [12] is also included (dotted line). The measured ranges actually extend to 17.9 Å^{-1} (HASYLAB) and 20.2 Å^{-1} (ESRF). The quality of the agreement between the different experiments is shown in figure 4.

from Narten and Levy's 20 year old results are probably related to our reduction of (possible) systematic errors in the multiple scattering and the other corrections. But the overall agreement of our curve with their data is excellent.

Equation (3) can be re-arranged to express the difference in structure factors between H_2O and D_2O

$$\Delta S_X(Q) = I_{H_2O}(Q) - I_{D_2O}(Q) = \Delta D(Q) + \Delta\langle F^2\rangle + \Delta C(Q) \tag{15}$$

where $\Delta D(Q)$ is the difference in the intermolecular structure factor, $\Delta\langle F^2\rangle$ is the difference in intramolecular scattering between light and heavy water and $\Delta C(Q)$ is the difference in Compton scattering between the two samples, which is negligible [1]. In the independent atom approximation, $\Delta\langle F^2\rangle$ is given by the difference in $\langle F^2\rangle$ of the isolated H_2O and D_2O molecules, calculated using equation (4) and the structural parameters of table 1. Such use of the independent atom model agrees with the electron diffraction results on the free molecule [13]. We have assumed that this result can be used for the liquid state, for which such results are unavailable. Using previously determined structural values for liquid water [9, 15], this calculation corroborates previous results for the H_2O–D_2O difference in which $\Delta\langle F^2\rangle$ was shown to be small compared to $\Delta S_X(Q)$ [1] as can be seen in figure 4.

In figure 4, the differences, $S_X(Q)$ of H_2O minus that of D_2O, are shown for all the experiments listed in table 2. The difference measurements from all experiments are in excellent agreement and therefore subsequent plots will show averaged differences at an effective temperature of 24.8 °C. There is a clear improvement in data quality and statistical accuracy compared to previous work [1]. Furthermore, the amplitude of the oscillations found in the new data is smaller than observed in the γ diffraction work by various amounts: the maximum amount being about a factor of two. In some places (e.g. $Q \simeq 2$ Å^{-1}) the error bars on the difference measurement of Root *et al* are somewhat smaller than the discrepancy with

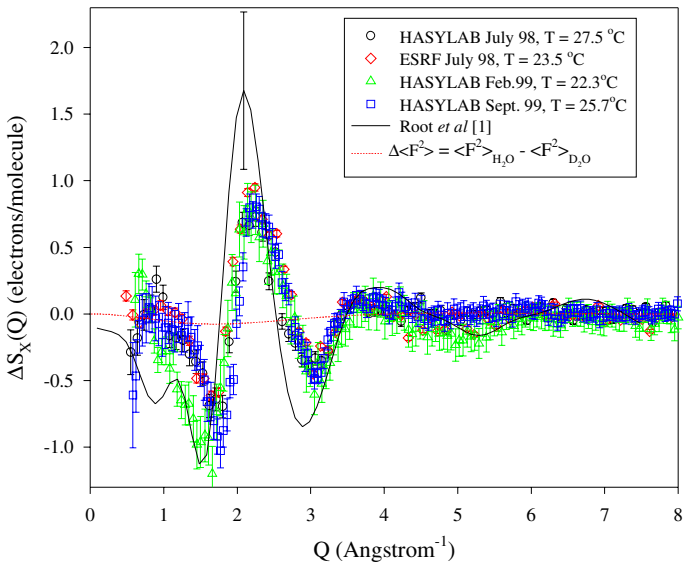

Figure 4. The measured isotopic difference, $\Delta S_X(Q)$ for H_2O minus D_2O from the experiments (see table 2) at HASYLAB (circles, triangles and squares) and ESRF (diamonds) with error bars. The data of Root *et al* [1] smoothed using a maximum entropy routine (solid line) is also included with one example of an error bar. The dotted line represents the calculated difference in form factors $\langle\Delta F^2\rangle = \langle F^2_{H_2O}\rangle - \langle F^2_{D_2O}\rangle$ obtained using the independent atom approximation [12].

the synchrotron work, which may be related to the normalization of $S(Q)$ in that work [26]. However, we note that there is qualitative agreement in the shape of the old and new isotopic difference measurements on water.

A careful review of the laboratory procedures and analysis for the ESRF experiment suggests the possibility that there was a slight shift in the tube centre between the empty vessel and sample plus vessel scans. This would lead to a spurious slope in $\Delta S_X(Q)$ measured at the ESRF. To correct for this effect, the $S_X(Q)$ for H_2O measured at ESRF was multiplied by a factor of 1.0075. The fact that the introduction of this factor significantly reduced Fourier transform artefacts in $\Delta g_X(r)$ and slightly improved the agreement with the HASYLAB data was an additional justification.

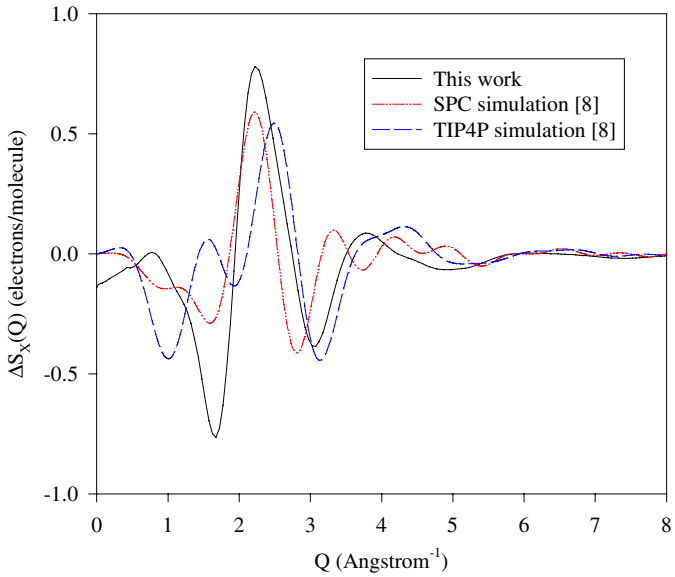

Figure 5. Maximum entropy fits to the four $\Delta S_X(Q)$ experiments (one at ESRF and three at HASYLAB) were averaged and the result is given by the solid line (average temperature 25.5 °C). This result is compared to the quantum simulation results using the SPC (dash–dot line) and TIP4P (dashed line) potential, both calculated by Del Buono *et al* [8] which both use the ST2 model potential. These theoretical results include only intermolecular effects.

In figure 5 the ESRF and HASYLAB difference measurements from figure 4 have been smoothed, averaged and compared to results for light water minus heavy water using either the SPC or TIP4P model potentials in a Feynman path-integral simulation at 25 °C to calculate the quantum contributions from isotopic differences in ground state librations [8]. The simulated results shown in figure 5 are Fourier transforms (equation (8) of [14]) of digitized data from graphs presented in the paper [8] of Del Buono *et al*. In this simulation study, intramolecular vibration modes and intermolecular exchange interactions were omitted. The main quantum contributions to the simulated structure came from zero-point motion of the molecules about the preferred hydrogen bond configuration [1, 4, 8].

In figure 6, similarly calculated quantum simulation results from other model potentials are compared to our synchrotron results. The ST2 [4, 8], and central force models [10] used in these calculations do not agree satisfactorily with the measured results, as their amplitudes are greater than observed. Although the central force model potential [10] was an adaptation of the ST2 model, its predictions differ markedly from the ST2 results shown in figure 6. Although

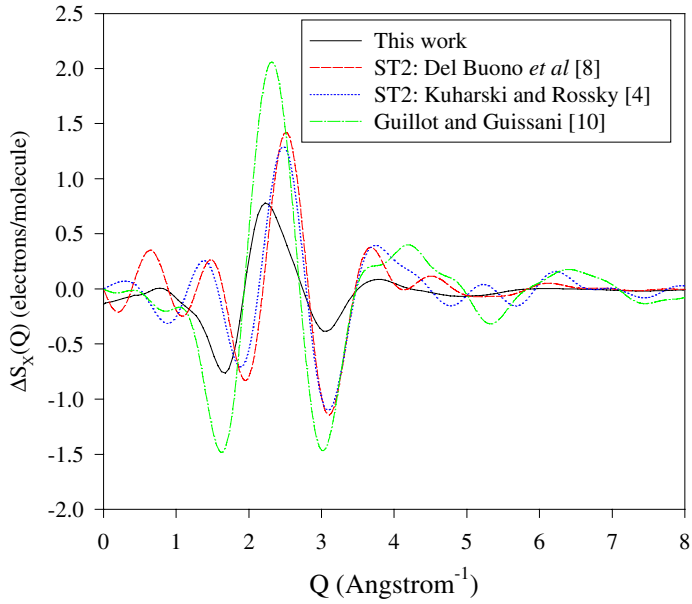

Figure 6. The solid line is the same averaged fit for $\Delta S_X(Q)$ as in the solid line in figure 5. This result is now compared to simulation results using other model potentials. The dashed line is from the results of Del Buono *et al* using the ST2 model [8] and the dotted line is Kuharski and Rossky's result for the same potential [4]. The dash–dot line is a modified ST2 potential used by Guillot and Guissani [10]. These theoretical results include only intermolecular effects.

the simulated results based on the SPC and TIP4P potentials [4,8] shown in figure 5 agree better with our experimental results than the simulated results shown in figure 6 (ST2 and central force), it is apparent that the shape of the $\Delta S_X(Q)$ curve from the ST2 based models is more like the measured curve even though it has a somewhat different magnitude. We note that the maximum measured $\Delta S_X(Q)$ in figures 5 and 6 corresponds to a 1.6% change in the x-ray static structure factor, i.e. at the maximum in $\Delta S_X(Q)$, we observed $\Delta S_X(Q)/S_X(Q) = 0.016$. For comparison the density difference between light and heavy water at 27.5 °C is 0.30%, which corresponds in linear dimensions to a change of less than 0.1%.

The real space isotopic effect, $\Delta g_X(r)$ following equation (6), was obtained through a Fourier transformation of a maximum entropy fit [24] to the measured data truncated at a node in $i(Q)$ at 15 Å^{-1}, and is shown in figures 7 and 8. The effect can be separated into intra- ($r < 1.51$ Å), intra–inter- (1.51 Å $\leqslant r \leqslant$ 2.5 Å) and inter-molecular ($r > 2.5$ Å) parts. In figure 7, there is fair agreement between the measured intermolecular structure and the quantum simulation predictions [8] using the SPC and TIP4P potentials for $r > 3$ Å. In the simulation, the water molecule was treated as being rigid which suggests the observed effect for $r > 2.5$ Å is dominated by the increased motion (bending) about the hydrogen bonds within the intermolecular network [4, 8, 10]. We observe that the first intermolecular peak in $\Delta g_X(r)$ occurs at 3.35 Å, which is close to the minimum after the first peak in $g_{OO}(r)$ and to the second peak in $g_{OH}(r)$. We note that at low r neither the ITD nor the computer simulations include intramolecular effects, and consequently we should compare these curves in the range $r > 2.5$ Å.

We have noted that for $r < 2.5$ Å the intramolecular correlations were omitted from all simulated structure results. For this reason, the anticipated dip at the OH bond length of about 0.96 Å (see $\Delta\langle F^2\rangle$ in figure 7) in the Fourier transform of $\Delta\langle F^2\rangle$ calculated using

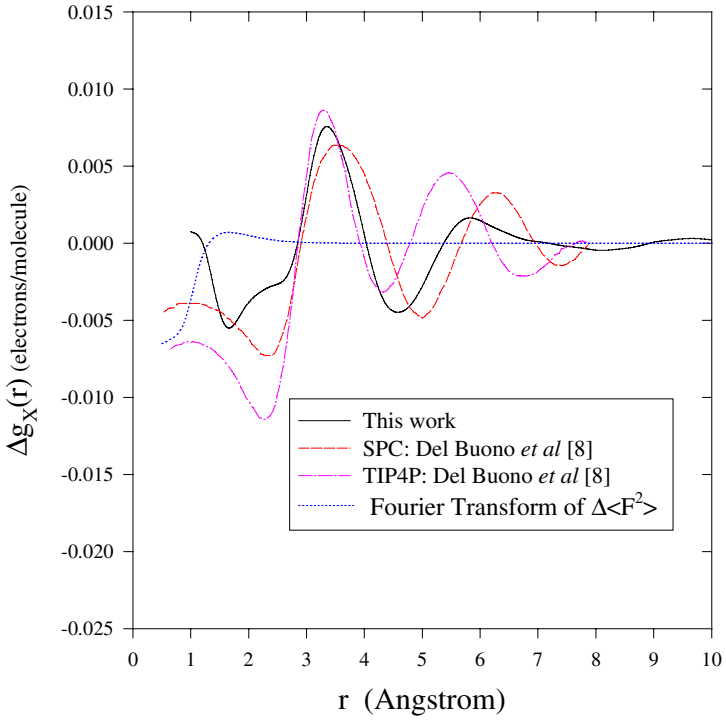

Figure 7. The solid line represents the measured $\Delta g_X(r)$ in real space, namely the Fourier transform of the solid line of figures 5 and 6. The intermolecular structural quantum effect predicted by the simulation of Del Buono *et al* [8] using the SPC model potential is shown by a dashed line and their TIP4P results [8] are shown by a dash–dotted line. The dotted line represents the Fourier transform of the dotted line in figure 4, that is, the single molecule isotopic difference. (The $r = 0$ limit for this function is zero and errors accumulate near this limit, consequently we have terminated all the data before this limit.)

equation (4) will be absent in the simulations. Although no contribution to the theoretical intramolecular calculation is expected beyond the maximum intramolecular distance in water (about 1.51 Å) and the simulation has no structural features below 2.5 Å, our measured $\Delta g_X(r)$ has a significant dip at 1.8 Å. This suggests the possibility that there is an isotopic difference in the intramolecular–intermolecular exchange interaction that was not included in the simulation studies. Hydrogen bonding studies of the water dimer predict an oxygen–oxygen mean distance of 2.85 Å [27] with the nearest neighbour oxygen situated on the OH bond axis. The mean intermolecular OH distance along the OH bond axis is $2.85 - 0.96 = 1.89$ Å. This is very near the position of our observed dip suggesting that it could be due to isotopic differences in the nearest neighbour hydrogen bond.

Figure 8 compares our measured results to simulated results using ST2C [4, 8] and central force [10] model potentials. The predictions from these Feynman path-integral simulations agree with the shape of our data but again differ from our amplitudes by about a factor of two. However, we note that the data of [10] are in better agreement with the experimental data of Root *et al* [1].

Following Root *et al* (figure 1) our figure 9 shows a comparison of the measured isotopic difference to that calculated using the isochoric temperature derivatives (ITD) of D_2O measured by Bosio *et al* [28] about a mean temperature of 11.2 °C. The absence of

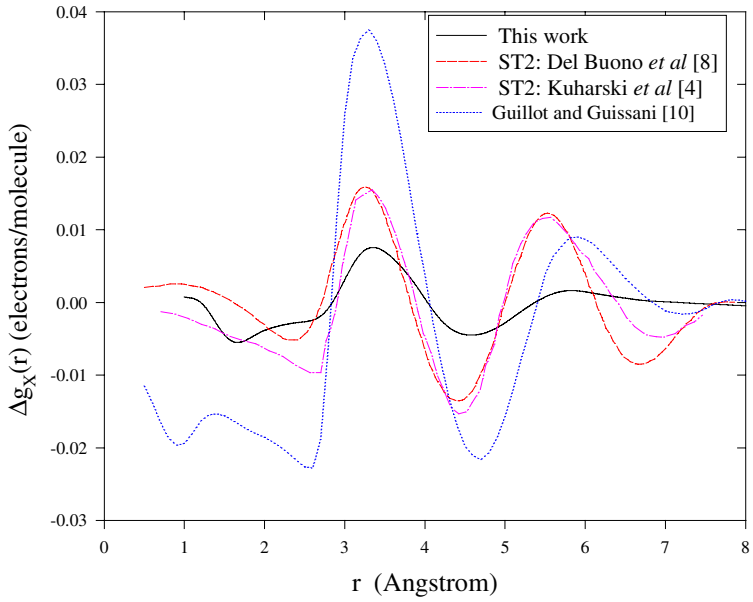

Figure 8. The solid line represents the average measured $\Delta g_X(r)$. The intermolecular structural quantum effect predicted by the simulation of Del Buono *et al* [8] is shown by a dashed line and Kuharski and Rossky's results [4] are shown by a dotted line, both for the ST2 potential. Guillot and Guissani's [10] results are shown by a dash–dot line. (The $r = 0$ limit for this function is zero and errors accumulate near this limit, consequently we have terminated all the data before this limit.)

any structure below 2.8 Å in the temperature derivative is due to the fact that differences in the intramolecular structure of a molecule due to the change in temperature are negligible. However, the intermolecular H_2O–D_2O difference at room temperature is well approximated by a temperature difference in D_2O of 5.5 °C (about a mean of 11.2 °C) at constant D_2O density. This is consistent with the idea that H_2O is more disordered than D_2O at the same temperature which previous workers have attributed to the softening of the H_2O peaks relative to the D_2O peaks by increased zero-point motions [1].

6. Conclusions

Precise high energy synchrotron radiation experiments at ESRF and HASYLAB have demonstrated a change of up to 1.6% in the static structure factor of water at room temperature caused by hydrogen-deuterium substitution (see figure 7). These results depend upon the high accuracy (±0.1%) that can be obtained using this technique. This is partly due to the high intensity of the beam and partly due to the use of small samples and small angles of scatter which minimize the experimental corrections. These data verify approximately the magnitude of the intermolecular structural effect found in quantum-mechanical simulations with the SPC and TIP4P potentials. However our experimental results include both the inter- and intramolecular effects.

We note that qualitative agreement is obtained with quantum simulations using the ST2 and central force models as well as with the previous measurements of Root *et al* [1]. Comparison of simulated results to the previous measurements of Root *et al* [1] had suggested that the

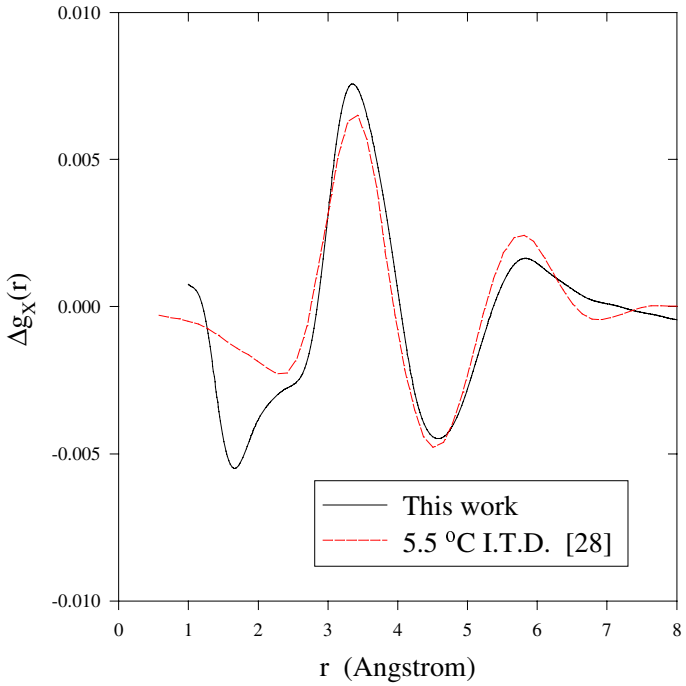

Figure 9. The solid line represents the average measured $\Delta g_X(r)$. The dotted line represents the structural difference produced by a 5.5 °C temperature shift (centred about 11.2 °C) as predicted using the isochoric temperature derivatives of Bosio *et al* [28]. For $r < 2.5$ Å there is a difference due to the fact that our work includes intramolecular effects, but to a first approximation the temperature derivative does not.

central-force model potential [10] produced the best agreement to measured results. However in our work, using small vessels to reduce multiple scattering and background and profiting from the use of world class high flux, high energy photon sources, the new data have clearly indicated that the SPC and TIP4P model potentials estimate the intermolecular structural quantum effect more accurately than any of the three models listed in figure 8. The increased quantum-mechanical motions of the lighter hydrogen atom compared to the deuterium atom have been shown by these simulations to soften the intermolecular structure producing the observed isotopic effect for $r > 2.5$ Å. The shape and magnitude of the effect over this region are well reproduced by temperature difference data using $\Delta T = 5.5$ °C, calculated from the temperature derivatives at constant density for D_2O measured by Bosio *et al* about a temperature of 11.2 °C. We hope that data of this kind will allow improvements in the design of neutron scattering experiments to determine the structure in hydrogenous compounds with a higher degree of precision.

Although the measured quantum difference also includes many body effects, nearly all of the theoretical pair potential models available are in fact effective pair potentials. In these theoretical models, the pair potential is adjusted to produce the best agreement with experimental results thus partly including many body effects [4, 10, 29] and some quantum-mechanical effects implicitly. It is notable that intramolecular effects have been omitted from these calculations. Thus, the agreement between our experimental data and theoretical predictions for $r > 2.5$ Å is a combined check upon the choice of pair potential and the corresponding approximations made for many body effects. The fact that the theoretically

calculated isotopic effect is found to depend on the potential model is strongly suggestive that a more theoretically rigourous calculation is necessary in which the quantum mechanical effects are fully coupled to the pair potential. Furthermore, the presence of isotopic structural differences in the neighbourhood of 2 Å, which is greater than the maximum intramolecular distance, was not predicted in any of the simulations studied. This may conflict with one assumption used in the simulations: that (to a first approximation in water) ground state intramolecular effects can be decoupled from those of intermolecular librations. A further study of structure for $r < 2.5$ Å is required. However, the commonly used time saving approximations in many simulations can be tested using *ab initio* Carr–Parrinello simulations that are now feasible with the latest generations of powerful computing devices. It is hoped that our experimental results will be useful in comparisons with such simulations and others using various new methods.

Acknowledgments

Staff at the Hamburger Synchrotronstrahlungslabor HASYLAB and the European Synchrotron Radiation Facility ESRF are thanked for providing the apparatus and the beamtime, and their assistance in conducting the experiments. The work of the Canadian participants was supported by a grant from NSERC Canada. Professor A K Soper is thanked for many useful discussions of the x-ray data.

References

[1] Root J H, Egelstaff P A and Hime A 1986 *Chem. Phys.* **109** 5164
[2] Melting points 0.00 °C for H_2O and 3.82 °C for D_2O. Boiling points 100.00 °C for H_2O and 101.42 °C for D_2O. These values were taken from
Lide D R (ed) 1998–9 *CRC Handbook of Chemistry and Physics* 79th edn
[3] Nemethy G and Scheraga H A 1964 *J. Chem. Phys.* **41** 680
[4] Kuharski R A and Rossky P J 1985 *J. Chem. Phys.* **82** 5164
[5] Narten A H and Levy H A 1975 *Water: a Comprehensive Treatise* vol 1, ed F Franks (London: Plenum) ch 8
[6] Soper A K 1984 *Chem. Phys.* **88** 187
[7] Sette F, Ruocco G, Krisch M, Bergmann U, Masciovecchio C, Mazzacurati V, Signorelli G and Verbeni R 1995 *Phys. Rev. Lett.* **75** 850
[8] Del Buono G S, Rossky P J and Schnitker J 1991 *J. Chem. Phys.* **95** 3728
[9] Frank H 1972 *Water: a Comprehensive Treatise* ed F Franks (London: Plenum) p 515
[10] Guillot B and Guissani Y 1998 *Fluid Phase Equilibria* **150–151** 19–32
[11] Egelstaff P A 1992 *An Introduction to the Liquid State* 2nd edn (Oxford: Clarendon) ch 3
[12] Hubbell J H, Veigele W J, Briggs E A and Howerton R J 1973 *J. Phys. Chem. Ref. Data* **4** 471
[13] Shibata S and Bartell L S 1965 *J. Chem. Phys.* **42** 1147
[14] Narten A H and Levy H A 1971 *J. Chem. Phys.* **55** 2263
Narten A H 1970 1995 *ORNL* Report 4578
[15] Kern C W and Karplus M 1972 *Water: a Comprehensive Treatise* ed F Franks (London: Plenum) p 21
[16] Robinson G W, Zhu S, Singh S and Evans M W 1996 *Water in Biology, Chemistry and Physics* (Singapore: World Scientific)
[17] Klein O and Nishina Y 1929 *Z. Phys.* **57** 853
[18] Guinier A 1963 *X-Ray Diffraction* (Saj Francisco: Freeman)
[19] Bouchard R, Hupfeld D, Lippmann T, Neuefeind J, Neumann H-B, Poulsen H F, Rütt U, Schneider J R, Süssenbach J S and Zimmermann M v 1998 *J. Synchrotron Radiat.* **5** 90
[20] Poulsen H F, Neuefeind J, Neumann H-B, Schneider J R and Zeidler M D *J. Non-Cryst. Solids* **188** 63
[21] Egelstaff P A 1986 *Methods of Experimental Physics: Neutron Scattering* ed D L Price and K Sköld (New York: Academic) p 444
[22] Soper A K and Egelstaff P A 1980 *Nucl. Instrum. Methods* **178** 415
[23] Palman H H and Pings C J 1962 *J. Appl. Phys.* **33** 2635
[24] Soper A K, Andreani C and Nardone M 1993 *Phys. Rev.* E **47** 2598

[25] Kell G S 1972 *Water: A Comprehensive Treatise* ed F Franks (London: Plenum) p 379
[26] Root J H 1986 Quantum effects in the structure of water *PhD Thesis* University of Guelph
[27] Rao C N R 1972 *Water: A Comprehensive Treatise* ed F Franks (London: Plenum) p 93
[28] Bosio L, Chen S and Teixeira J 1983 *Phys. Rev. Lett.* A **27** 1468
[29] Egelstaff P A 1983 *Physica* B **120** 335